





Elastic hoops jumping on water

Han Bi Jeong ^{1,*}, Ji-Sung Park ^{1,*}, Eunjin Yang,² Yunsuk Jeung ¹,
Juliette Amauger,³ and Ho-Young Kim ^{1,4,†}

¹*Department of Mechanical Engineering, Seoul National University, Seoul 08826, Korea*

²*Korea Institute of Science and Technology Evaluation and Planning, Seoul 06775, Korea*

³*Département de Physique, Ecole Normale Supérieure, PSL Research University,
24 rue Lhomond, 75005 Paris, France*

⁴*Institute of Advanced Machines and Design, Seoul National University, Seoul 08826, Korea*



(Received 15 June 2023; accepted 28 August 2023; published 20 October 2023)

Although the mechanics of jumping on water dominated by surface tension are well established, the understanding of water jumping dominated by drag force, as observed in organisms like fishing spiders, remains incomplete despite its potential to achieve high jumping velocity. Here, we demonstrate that simple elastic hoops can achieve drag-dominated jump on water, and use this model system to construct a fundamental framework to theoretically analyze jump dynamics propelled by form drag. In addition to numerically solving the hoop trajectory while interacting with water, we show that the take-off velocity scaled by the hoop's free vibration velocity depends solely on the solid-fluid density ratio. A comparison with hoop jumps on solid ground reveals that the hoop jumps on water are delayed with a lower jumping efficiency. This work can not only contribute to the development of efficient and easily constructible biomimetic robots but also provide a foundation for understanding the optimal design principles and evolutionary pressures that shape biological jumpers.

DOI: [10.1103/PhysRevFluids.8.100503](https://doi.org/10.1103/PhysRevFluids.8.100503)

I. INTRODUCTION

Locomotions of biological creatures on the surface of water have been actively studied for decades, whose examples include skating [1], meniscus climbing [2], and jumping [3–5] of semi-aquatic arthropods, running of basilisk lizards [6], and walking of dolphins. In particular, arthropods such as springtails [7,8], water striders [3], and fishing spiders [5] jump on water to escape predators approaching from below the water surface. For an animal to jump on the water, upward momentum provided by the water should be large enough to launch the creature in the air, a rare feat defying our common notion that water is easily breakable. The forces from water generated as the reaction to the driving stroke of jumping animals can come from surface tension, buoyancy, drag, and added inertia.

It is now well established that small insects like springtails and water striders, whose leg stroke speed is not high enough to induce significant hydrodynamic drag, rely on surface tension of water to jump [3,4]. A robotic insect emulating the surface-tension-dominated jumping was also demonstrated [9], exemplifying that biomimetic machines can help us to clearly understand the physical principle at work in the biological world. It was recently suggested that the drag-dominated jumpers can exhibit higher take-off velocity than surface-tension dominated ones owing to greater

*These authors contributed equally to this work.

†hyk@snu.ac.kr

TABLE I. Mechanical properties and thickness of the hoops.

Material	Density (kg/m ³)	Young's modulus (GPa)	Thickness (μm)
PI	1420	2.91	125
SUS	8000	190	50

momentum transferred to the water [10]. However, the detailed dynamics of the drag-dominated water jumps of either biological creatures, e.g., fishing spiders and pygmy mole crickets [11], or artificial robots [10] are still incomplete when compared to the level of our understanding on the surface-tension dominated jumping.

Here, we investigate the jumps on water thrust by hydrodynamic drag with an artificial model, an elastic hoop, whose jump dynamics on the ground was elucidated previously [12]. Its simple geometry and kinematics allow us to grasp detailed understanding of the jumping dynamics including the temporal evolution of wetted length and location of mass center, take-off velocity, and even the jumping efficiency. Using a jumper that can also work on ground allows us to find the difference of jump behavior on ground and water. Our artificial jumper not only can serve as an efficient yet easy-to-build biomimetic robot, but also will help us to build a model to understand its biological counterparts, whose optimal design principle and evolutionary pressure to shape them still await to be discovered.

In the following, we start with describing the experimental procedure to measure the jump of the artificial jumper. After clarifying the dominant force acting on the jumper and performing dimensional analysis, we mathematically model the hoop dynamics and compare our theoretical and experimental results. In addition to solving the differential equations, we discuss functional dependence of the take-off velocity on various parameters using dimensional analysis and physical arguments. We assess the jump efficiency of the elastic jumper based on our model, and conclude with discussing the implications of this work.

II. EXPERIMENTAL

The hoops, our model jumper, are made of thin strips of either polyimide (PI) or stainless steel (SUS 304) with 2 mm of width (b), which are bent and glued in circle with radius r_0 . The density (ρ_s), Young's modulus (E), and the thickness (τ) of PI and SUS strips are listed in Table I. The outer surfaces of the hoops are treated with superhydrophobic coating (Ultra-Ever Dry), to have the similar wetting condition as fishing spiders [13]. This super water repellency minimizes water-solid adhesion [14] and prevents breaking of water surface that can cause significant water splash and deterioration of jump efficiency. A cotton thread shorter than the hoop diameter deforms the circular hoop as shown in Fig. 1(a). Upon floating a hoop on water, an infrared laser (IRCL-1W-1064, CrystaLaser) burns the center of the thread to set the hoop into motion as its elastic strain energy is released.

The hoop is initially in a peanut shape with the waist length of $2r_0 - \delta$, but becomes elliptic instantaneously upon release to assume a shape as shown in Fig. 1(b). We vary the hoop radius r_0 from 10 to 18 mm and the initial deflection δ from $0.6r_0$ to r_0 . In Figs. 1(a) and 1(b), the height of the center of mass from the unperturbed free surface is denoted by y , and the distance from the lowest point on the vertical axis to the center of mass is denoted by l . We define $h = l - y$. We denote the angle from the vertical axis to an edge of the wetted length by α . At an arbitrary point on the wetted length with the angle from the vertical axis θ , the distance from the hoop center and the unperturbed free surface is respectively s and d . The subsequent motion of the hoop and water before and after takeoff, as shown in Fig. 1(c), are imaged by a high-speed camera (Fastcam SA-Z, Photron) running at a frame rate up to 4000 s^{-1} .

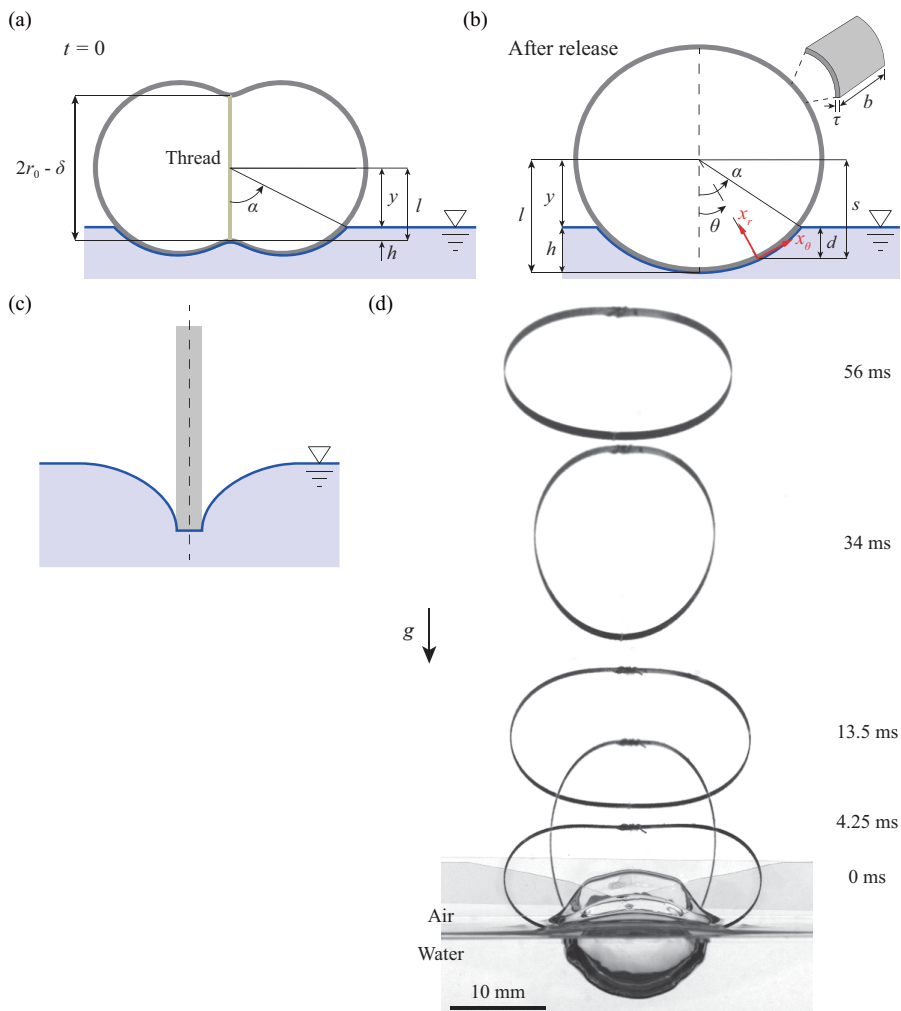


FIG. 1. (a) A schematic of the initial configuration of an elastic hoop floating on water. (b) The hoop shape during interaction with water. (c) Side view of the hoop. (d) Overlapped images of a SUS hoop of radius $r_0 = 14$ mm with the initial deformation $\delta = 14$ mm, which is set into motion at $t = 0$ upon laser cutting the thread and disengages from the water surface at $t = 3.5$ ms. The water images are also overlapped.

III. MODELING HOOP DYNAMICS ON WATER

We first consider the forces acting on the hoop before it disengages from the water in order to identify the dominant reaction force provided by water. On a floating body, the weight, F_g , buoyancy F_b and the surface tension force F_s act, whose magnitudes are respectively scaled as $F_g \sim 2\pi r_0 \tau b \rho_s g$, $F_b \sim \rho_f g b h l_w$, and $F_s \sim \sigma l_w$. Here, ρ_f is the water density, g is the gravitational acceleration, l_w is the wetted length ($\sim r_0$), and σ is the surface tension coefficient of water. As the hoop vibrates from the initially bent configuration, the wetted part experiences drag consisting of form drag F_d and viscous drag F_v , which are scaled as $F_d \sim \rho_f b l_w u_v^2$ and $F_v \sim \mu u_v l_w$. Here, u_v is the velocity of hoop bottom due to vibration and scaled as $(\delta/2)\omega_n$, where ω_n is the characteristic scale of the natural frequency of vibration for an elastic hoop [15, 16]: $\omega_n = (E/\rho_s)^{1/2} \tau/r_0^2$. In addition, the acceleration of the wetted part of the hoop induces the acceleration of the surrounding fluid,

requiring us to consider the added inertia, $F_a \sim \rho_f b \tau l_w a$ with a being the acceleration scaled as $a \sim (\delta/2)\omega_n^2$.

For the hoops used in our experiments, whose properties and dimensions are given above, we find the force ratios relative to drag are such that $F_g/F_d \sim 10^{-2}$, $F_b/F_d \sim 10^{-2}$, $F_s/F_d \sim 10^{-2} - 10^{-1}$, $F_v/F_d \sim 10^{-3}$, and $F_a/F_d \sim 10^{-2}$. It implies that the form drag dominates the reaction of water to the hoop motion, and thus we neglect the other forces in our model. Then the take-off velocity of a hoop from the water surface, u_t , must be a function of the following variables: E , ρ_f , ρ_s , C_d , τ , r_0 , and δ . Here, C_d is the drag coefficient of the hoop bottom defined as $C_d = 2F_d/(\rho_f b l_w u_v^2)$. Dimensional analysis [17,18] reveals that the dimensionless take-off velocity $u_t/(E/\rho_s)^{1/2}$ depends on the following dimensionless parameters: ρ_s/ρ_f , C_d , τ/r_0 , and δ/r_0 .

Because the hoop moves upon release from its compressed state by vibration, the intrinsic velocity scale in this problem is given by the characteristic vibration velocity: $u_v = (\delta/2)\omega$. Here, ω is the damped natural frequency of a floating hoop. Our experiments with various sizes of PI and SUS hoops that float on water reveal that ω can be expressed as $\omega = \gamma\omega_n$ with $\gamma = 0.55$. We now seek functional dependency of a scaled take-off velocity $u_t/u_v = 2u_t r_0^2 / [(E/\rho_s)^{1/2} \gamma \tau \delta]$ on dimensionless parameters. Our dimensional analysis above now tells us that u_t/u_v depends only on the solid-fluid density ratio ρ_s/ρ_f as long as C_d is constant: $u_t/u_v = f(\rho_s/\rho_f)$. To go beyond these scaling estimates and analytically describe the hoop dynamics, we compute the location of the hoop's center of mass as a function of time and take-off velocity in the following.

We start from the equation of motion for a hoop of mass m that pushes the water surface over a wet arc, $-\alpha < \theta < \alpha$, to experience an external force due to form drag:

$$m\ddot{y} = \int_{-\alpha}^{\alpha} \frac{1}{2} C_d \rho_f b r u^2 d\theta, \quad (1)$$

where $\ddot{y} = d^2y/dt^2$ with t being time and $u(\theta, t)$ the local downward velocity of hoop pushing the water surface. We assume $r = r_0$ to simplify our evaluation of the arc length as the hoop vibrates. For example, the initial wet length of a SUS hoop of $r_0 = \delta = 14$ mm was measured to be 27 mm with $\alpha = 58^\circ$, which is only 5.6% shorter than the circular arc length with the same r_0 and α . We estimate the value of C_d for the floating strip, which pushes water in the front while exposed to air in the rear, using that of a fully submerged semicircular nose section, $C_d = 1.16$ [19]. It is because both of them confront water in the frontal curved surface but experience insignificant pressure variation in the rear.

To solve Eq. (1) for y , we need information of u as a function of θ and t , and α as a function of t . The experimental images of a hoop starting its motion at $t = 0$ on the water surface, Fig. 2, show that the hoop goes through vibration of the second mode (prolate-oblate shape change). For a thin ring under such vibration, the radial and circumferential components of displacement are respectively written as $x_r(\theta, t) = 2B \cos 2\theta \cos(\omega t + \epsilon)$ and $x_\theta(\theta, t) = -B \sin 2\theta \cos(\omega t + \epsilon)$, where B is the vibration amplitude and ϵ is the phase adjustment to match the initial condition [20]. With $x_r(0, 0) = \delta/2$ and $x_r(\theta, \pi/(2\omega)) = 0$, we obtain $B = \delta/2$ and $\epsilon = 0$. Thus, we write $x_r(\theta, t) = (\delta/2) \cos 2\theta \cos \omega t$, $x_\theta(\theta, t) = -(\delta/4) \sin 2\theta \cos \omega t$, and $l = r_0 - (\delta/2) \cos \omega t$. The distance of a point in the wetted region from the center of mass, s , as indicated in Fig. 1(b), is $s = (r_0 - x_r) \cos \theta - x_\theta \sin \theta$, and its distance from the unperturbed free surface $d = s - y$. As the vertical component of the hoop velocity with respect to the center of mass is \dot{s} at θ , we get $u = \dot{d} = \dot{s} - \dot{y}$. Then Eq. (1) is written as

$$\ddot{y} = \frac{C_d \rho_f b r_0}{2m} \int_{-\alpha}^{\alpha} \left[\frac{\omega \delta}{2} \left(\cos 2\theta \cos \theta - \frac{1}{2} \sin 2\theta \sin \theta \right) \sin \omega t - \dot{y} \right]^2 d\theta. \quad (2)$$

We can relate y to α because the value of s when $\theta = \alpha$ corresponds to y :

$$y = r_0 \cos \alpha - \frac{\delta}{2} \left(\cos 2\alpha \cos \alpha - \frac{1}{2} \sin 2\alpha \sin \alpha \right) \cos \omega t. \quad (3)$$

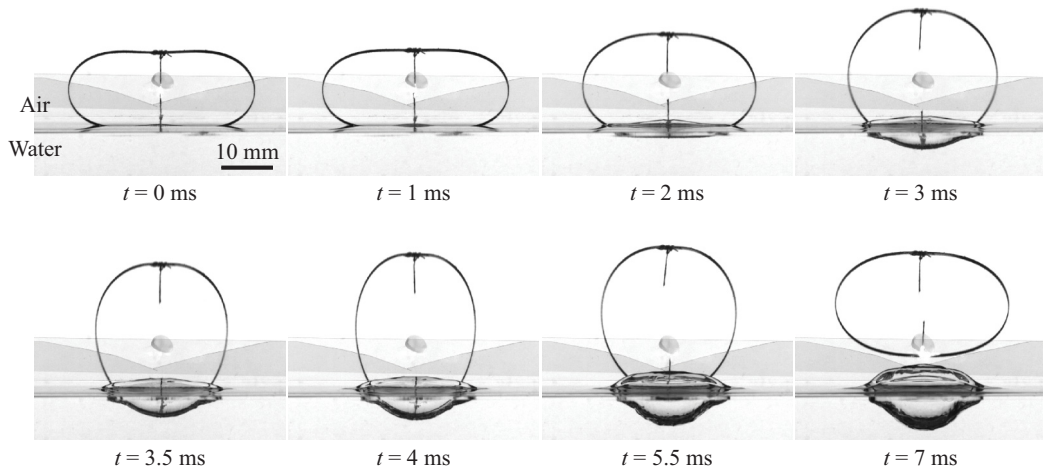


FIG. 2. Interaction of the vibrating elastic hoop shown in Fig. 1(c) with the water surface. The initially oblate hoop pushes the water surface by vibration, so that the hoop bottom moves downward initially. As the center of mass of the hoop rises because of the upward thrust provided by the water drag, the hoop bottom eventually stops descending but begins rising, corresponding to takeoff ($t = 3.5$ ms). The hoop then rises into the air while continuing vibration.

Differentiating Eq. (3) with respect to t twice, we get the following differential equation:

$$\ddot{y} + G_1\ddot{\alpha} + G_2\dot{\alpha}^2 + G_3\dot{\alpha} + G_4 = 0, \quad (4)$$

where

$$G_1 = \omega^2 \left[r_0 \sin \alpha + \frac{\delta}{4} \cos \omega t (-4 \sin \alpha \cos 2\alpha - 5 \cos \alpha \sin 2\alpha) \right], \quad (5)$$

$$G_2 = \omega^2 \left[r_0 \cos \alpha + \frac{\delta}{4} \cos \omega t (13 \sin \alpha \sin 2\alpha - 14 \cos \alpha \cos 2\alpha) \right], \quad (6)$$

$$G_3 = \omega^2 \frac{\delta}{2} \sin \omega t (4 \sin \alpha \cos 2\alpha + 5 \cos \alpha \sin 2\alpha), \quad (7)$$

$$G_4 = \omega^2 \frac{\delta}{4} \cos \omega t (\sin \alpha \sin 2\alpha - 2 \cos \alpha \cos 2\alpha). \quad (8)$$

Simultaneously solving the two second-order differential equations, Eqs. (2) and (4), with the initial conditions of $y(0) = y_i$, $\dot{y}(0) = 0$, $\alpha(0) = \alpha_i$, and $\dot{\alpha}(0) = 0$, yields y and α as functions of time. The initial values of $y_i = l(0) - h(0)$ and α_i are a consequence of the balance of hoop weight and hydrostatic force from buoyancy and surface tension. The characteristic depression of the water surface, \hat{h} , because of the hoop weight can be scaled as $\hat{h} \sim (\rho_s/\rho_f)\tau$ using Keller's theorem [21] stating that the weight of the displaced water volume by the floating solid and deformed meniscus ($\sim \rho_f g \hat{h} r_0 b$) is equal to the solid weight ($2\pi \rho_s g r_0 b \tau$). In our experimental conditions, $\hat{h} < r_0/10$, and we use the experimentally measured values of $l(0)$ and $\alpha(0)$ to get y_i . We numerically calculate y and α as time marches, and find the take-off velocity at the moment the hoop bottom no longer descends but rises.

IV. RESULTS

Figures 3(a)–3(d) plot typical trajectories of a SUS hoop as a function of time before takeoff. We see in Fig. 3(a) that the experimentally measured hoop bottom's relative distance from the center of mass follows the sinusoidal curve, $l = r_0 - (\delta/2) \cos \omega t$. While the hoop keeps extending vertically

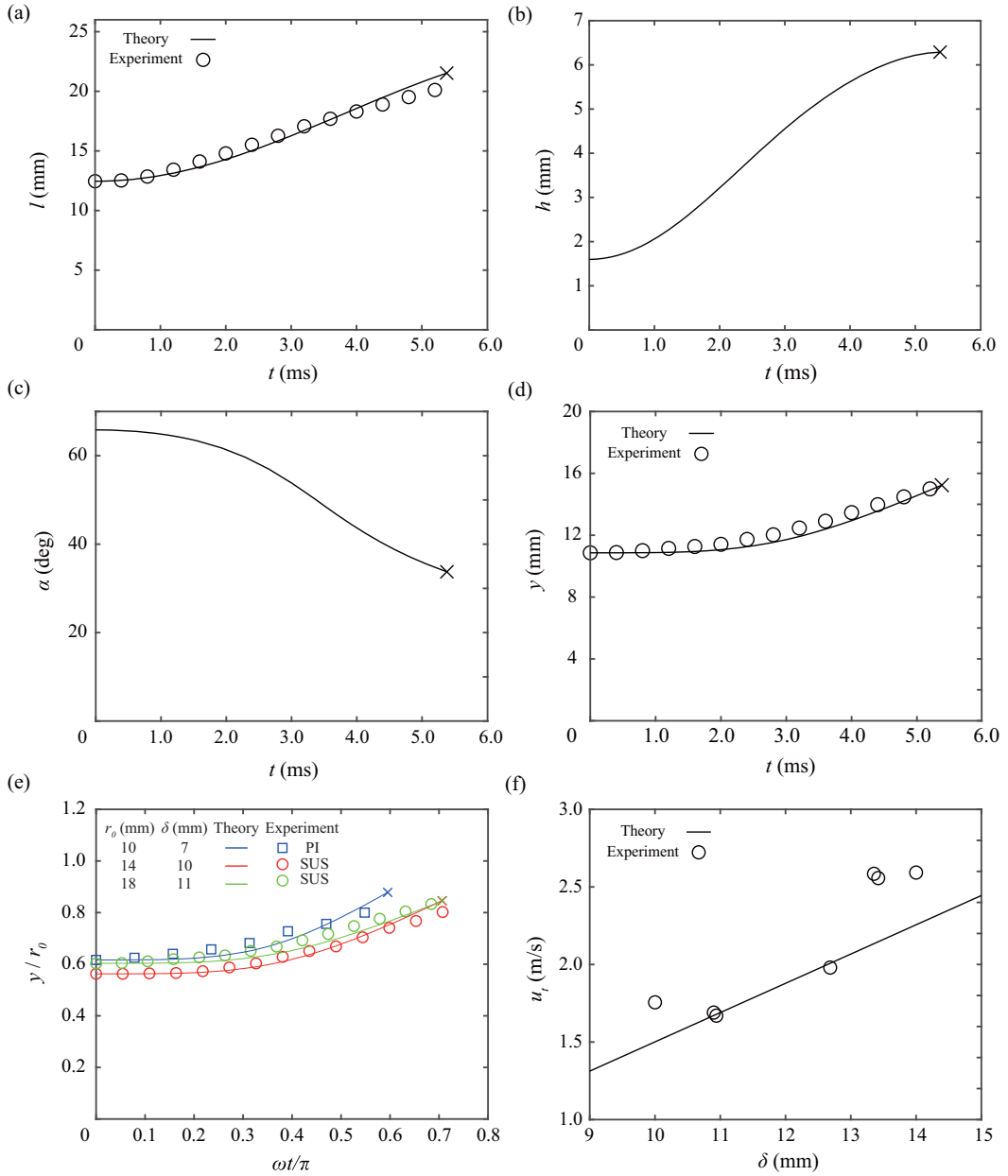


FIG. 3. (a) Hoop bottom’s relative distance along the vertical axis from the center of mass, l , versus time. The solid line corresponds to $l = r_0 - (\delta/2) \cos \omega t$. (b) Hoop bottom’s depth from the unperturbed free surface, h , versus time. (c) The half central angle of wetted portion of hoop, α , versus time. (d) The height of center of mass from the unperturbed free surface, y , versus time. For (a)–(d), a SUS hoop of radius $r_0 = 18$ mm with the initial deformation $\delta = 11.2$ mm was used. (e) Dimensionless height of the center of mass, y/r_0 , versus the dimensionless time, $\omega t/\pi$, for various hoops. (f) Theoretical take-off velocity of SUS hoops of $r_0 = 14$ mm as a function of the initial deflection δ .

to change from oblate to prolate configuration by vibration, the hoop bottom tends to push the water surface down, as shown in the first row of Fig. 2 and the increasing depth of hoop bottom, h , in Fig. 3(b). However, the half central angle of the wetted arc, α , in Fig. 3(c) shows that α decreases

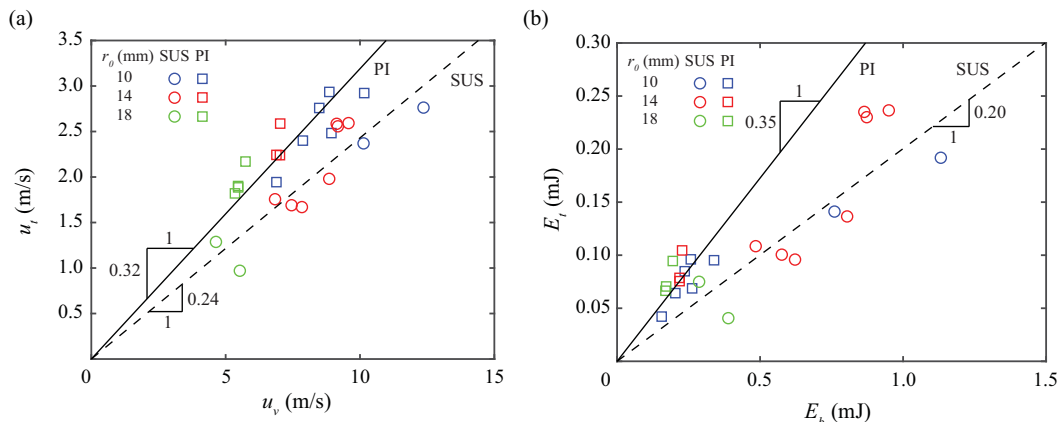


FIG. 4. (a) Take-off velocity u_t versus the characteristic vibration velocity u_v . Squares and circles correspond to experimental data and the solid lines are best fitting lines for each density ratio. (b) The translational kinetic energy versus the elastic strain energy. The slopes of the best fitting lines of each hoop material correspond to the jumping energy efficiency.

as the hoop grows more prolate with time. We only plot the computed results of h and α because the optical blurriness below the free surface prevents exact evaluation of the wet edge of the hoop through image analysis. Owing to the upward thrust provided by the water drag in reaction to the downward pushing of the hoop's wetted portion, the height of center of mass y keeps increasing, as shown in Fig. 3(d). We see that our theoretical prediction of y , assuming drag as the dominant force from water, match well with the experimental data.

We perform computation until the hoop bottom stops descending, or when $\dot{h} = 0$ in Fig. 3(b), which corresponds to takeoff. We indicate the moments of takeoff as crosses in Fig. 3. It is interesting to note in Fig. 3(c) that the hoop still touches the water surface over a finite angle until take-off occurs, in contrast with the case where a hoop compressed on the solid ground jumps. In such ground jumping, the hoop vibrating on the ground takes off when it becomes a perfect circle and makes a point contact with the ground [12].

Figure 3(e) shows the dimensionless height of center of mass, y/r_0 , versus dimensionless time, $\omega t/\pi$, for different hoop conditions. In addition to favorable agreement of our theory and experiment, we see that all the hoops take off when $\pi/2 < \omega t < (3/4)\pi$. This is also in contrast with the jumps on ground, where the hoops take off when ωt is exactly $\pi/2$ or when recovering a perfect circular shape [12]. The delay of takeoff on water in comparison to that on ground is caused by the fluidity of base that deforms and flows as the hoop's wet portion pushes down, resulting in a mismatch of oscillation frequencies of hoop and water, and the reduction of propulsive force. Thus, the dimensionless take-off times on water differ depending on hoop conditions.

Figure 3(f) plots the experimentally measured take-off velocity, u_t , of SUS hoops with a constant radius as a function of initial deflection. We also plot the theoretical calculation results for the corresponding conditions as solid lines. Both experiment and theory reveal that u_t tends to increase linearly with δ , with the maximum error of the simulation being 17% of the experimental data. The relatively large discrepancies between theory and experiment for large δ are supposed to come from geometric nonlinearity that falls beyond the hoop model of Love [20].

We now turn to the dimensional analysis, which has predicted above that the dimensionless take-off velocity u_t/u_v depends only on ρ_s/ρ_f , so that $u_t/u_v = f(\rho_s/\rho_f)$. Here $f(\rho_s/\rho_f)$ is a function of a single variable ρ_s/ρ_f , which can only be determined either by experiments or computations. Plotting the experimentally measured take-off velocity u_t of PI and SUS hoops versus the characteristic vibration velocity $u_v = (\delta/2)\omega$, in Fig. 4(a), we find u_t of each hoop material to be indeed linearly dependent on u_v with different slopes depending on ρ_s/ρ_f : $f(\rho_s/\rho_f) = 0.32$ for PI and 0.24 for SUS.

The jumping hoop converts the elastic strain energy stored in the initially deflected configuration into the kinetic energy associated with translational and vibrational motions. Here, we are interested in the conversion efficiency of the bending strain energy E_b to the translational energy at takeoff, E_t : $\eta = E_t/E_b$. It is known that the elastic strain energy of a hoop can be obtained by assuming the hoop as a spring [12,20] with the spring constant of $k = 0.56Eb\tau^3/r_0^3$: $E_b = k\delta^2/2$. As the translational kinetic energy is given by $E_t = mu_t^2/2$, we find $\eta = 3.39f^2(\rho_s/\rho_f)$. Namely, the jumping efficiency depends only on ρ_s/ρ_f while being independent of E , and geometric parameters such as r_0 , τ , and δ . We find $\eta_P = 0.35$ and $\eta_S = 0.20$ for PI and SUS hoops, respectively, regardless of their radius, thickness, and initial deflection as long as the drag is a dominant reaction force to the hoop vibration and $C_d = 1.16$. Figure 4(b) plots the experimental kinetic energy based on the measured take-off velocity versus the initial strain energy. The empirical data of each material indeed tend to gather on straight lines with the slopes η_P and η_S , as theory predicts.

The insensitiveness of the jump efficiency to the hoop's elastic properties and dimensions is because the take-off velocity is scaled as the elastic vibration velocity of hoop. We note that on the rigid ground, the jump efficiency was found to be a constant of 0.57 for the absence of the effects of the base [12]. The water jumping efficiency is lower than the jumping efficiency on ground, implying significant energy loss due to energy transfer to water as well as to vibration. When the liquid density is lower, which results in a higher ρ_s/ρ_f , the form drag gets weaker, leading to a lower jump efficiency. In addition, the jump efficiency decreases as the solid density increases because much energy is required to set heavy hoops into motion.

We further note that the robotic insect's jump on water dominated by surface tension exhibits the same jumping efficiency as its jump on ground [9]. This implies that as long as the jumper uses the water as a springboard without breaking the water surface and causing too much flow, the water does not need to be considered as a mere damping medium. In the current drag-dominated jumps, however, the pressure difference of the wet front and dry rear sides of the floating strip is supposed to be a major source of reaction force, making the water as a damping medium. Although the jump efficiency might be lower for drag-dominated jumps than for surface-tension-dominated jumps, the jump height can be greater for drag-dominated jumps [10] because stronger momentum (thanks to high actuation velocity) can be transferred to water without worrying about breaking the water surface.

V. CONCLUSIONS

In summary, we have shown that centimetric elastic hoops simply made by bending and gluing thin strips can jump on water as thrust by form drag. These simple mechanical models convert the initial strain energy into damped free vibration, so that a wetted portion pushes the water surface to generate sufficient form drag to launch the hoop in the air. Without resorting to complicated design and fabrication of light-weight actuators, the elastic hoops allow us to mimic drag-based jumping of semi-aquatic arthropods like fishing spiders. The dynamic modeling of hoop motion based on the hoop vibration equation and Newton's second law of motion resulted in the temporal evolution of the height of hoop center that is consistent with experimental measurements. Therefore, this work presents a fundamental framework to mimic and understand drag-based water jumpers, which can be extended to both natural and artificial jumpers with more delicate designs.

We conclude by discussing the advantages, limits, and implications of our experimental system and theoretical model. Our jumpers, elastic hoops, are convenient to fabricate and model mainly because the elastic strip can both store and release energy, or can act as both an energy storage device and actuator. The hoop vibration resulting from the interconversion between strain and kinetic energy can be modeled by theory of elasticity. The theory allows us to obtain the functional dependency of the undamped natural frequency (ω_n) on various parameters, but we need separate experiments to find the damped natural frequency (ω), which determines how the hoop actuates. This is equivalent to previous research describing the appendage motion with respect to the water surface *a priori* in order to find the trajectory of water jumpers [3,4,9]. An intensive computational

model for the floating elastic hoop's motion accounting for the local fluid-structure interaction (FSI) of the infinitesimal section of hoop with surrounding water flow may eliminate the need of measuring ω , and allow the evaluation of energy transfer to water. However, here we employed measured values of ω and used an integral approach, Eq. (1), so as to focus on the drag-dominant jump principle and the hoop trajectory.

A comparison between hoop jumps on water using the form drag and on rigid ground has allowed us to uncover the impact of a fluid medium on jump dynamics. Notably, the take-off is delayed, and the jump efficiency is lower when jumping on water in comparison to jumps on solid ground. Besides the evident effects of water, which deforms and flows in response to the hoop's pushing force, we found that the jump efficiency on water is influenced by the ratio of solid-fluid densities, whereas it remains constant (0.57) on the ground. Lighter hoops exhibit higher jump efficiency on water, leading to PI hoops outperforming SUS hoops despite PI's low elastic modulus. This guides us to speculate that weight reduction plays a more significant role for aquatic jumpers compared to terrestrial jumpers, offering an intriguing perspective for understanding the biological design principles of aquatic jumpers and for consideration in the design of jumping robots.

Now that we have models for the surface-tension-dominated jump [3,9] and the drag-dominated jump on water, it is natural to proceed to consider a regime where both the surface tension and the drag are important, i.e., when the Weber number, $We = \rho_f u^2 b / \sigma$, is of the order of unity [22]. Experiments using our hoops with reduced initial deformation, elastic modulus, thickness, and width may allow us to investigate the corresponding regime. Understanding of such jumps would require us to take into account the deviation of meniscus shape from the static shape due to flow, beyond mere superposition of capillary and drag forces, which presents a complicated but worthy topic of further research.

ACKNOWLEDGMENTS

This work was supported by the National Research Foundation of Korea (Grants No. 2018-052541 and No. 2021-017476) via SNU SOFT Foundry. Administrative support from the SNU Institute of Engineering Research is gratefully acknowledged.

-
- [1] D. L. Hu, B. Chan, and J. W. M. Bush, The hydrodynamics of water strider locomotion, *Nature (London)* **424**, 663 (2003).
 - [2] D. L. Hu and J. W. M. Bush, Meniscus-climbing insects, *Nature (London)* **437**, 733 (2005).
 - [3] E. Yang, J. H. Son, S. Lee, P. G. Jablonski, and H.-Y. Kim, Water striders adjust leg movement speed to optimize takeoff velocity for their morphology, *Nat. Commun.* **7**, 13698 (2016).
 - [4] H.-Y. Kim, J. Amauger, H.-B. Jeong, D.-G. Lee, E. Yang, and P. G. Jablonski, Mechanics of jumping on water, *Phys. Rev. Fluids* **2**, 100505 (2017).
 - [5] R. B. Suter, Spider locomotion on the water surface: Biomechanics and diversity, *J. Arachnol.* **41**, 93 (2013).
 - [6] J. W. Glasheen and T. A. McMahon, A hydrodynamic model of locomotion in the basilisk lizard, *Nature (London)* **380**, 340 (1996).
 - [7] J. Brackenbury and H. Hunt, Jumping in springtails: Mechanism and dynamics, *J. Zool.* **229**, 217 (1993).
 - [8] S. Sudo, T. Kainuma, T. Yano, A. Shirai, and T. Hayase, Jumps of water springtail and morphology of the jumping organ, *J. JSEM* **15**, s117 (2015).
 - [9] J.-S. Koh, E. Yang, G.-P. Jung, S.-P. Jung, J. H. Son, S.-I. Lee, P. G. Jablonski, R. J. Wood, H.-Y. Kim, and K.-J. Cho, Jumping on water: Surface tension-dominated jumping of water striders and robotic insects, *Science* **349**, 517 (2015).
 - [10] M. Gwon, D. Kim, B. Kim, S. Han, D. Kang, and J.-S. Koh, Scale dependence in hydrodynamic regime for jumping on water, *Nat. Commun.* **14**, 1473 (2023).

- [11] M. Burrows and G. P. Sutton, Pygmy mole crickets jump from water, *Curr. Biol.* **22**, R990 (2012).
- [12] E. Yang and H.-Y. Kim, Jumping hoops, *Am. J. Phys.* **80**, 19 (2012).
- [13] R. B. Suter, G. E. Stratton, and P. R. Miller, Taxonomic variation among spiders in the ability to repel water: Surface adhesion and hair density, *J. Arachnol.* **32**, 11 (2004).
- [14] D.-G. Lee and H.-Y. Kim, The role of superhydrophobicity in the adhesion of a floating cylinder, *J. Fluid Mech.* **624**, 23 (2009).
- [15] R. Hoppe, The bending vibration of a circular ring, *Crelle J. Math.* **73**, 158 (1871).
- [16] J. L. Lin and W. Soedel, On general in-plane vibrations of rotating thick and thin rings, *J. Sound Vib.* **122**, 547 (1988).
- [17] E. Buckingham, On physically similar systems; Illustrations of the use of dimensional equations, *Phys. Rev.* **4**, 345 (1914).
- [18] A. A. Sonin, A generalization of the Π -theorem and dimensional analysis, *Proc. Natl. Acad. Sci. USA* **101**, 8525 (2004).
- [19] F. M. White, *Fluid Mechanics*, 4th ed. (McGraw-Hill, New York, 1999).
- [20] A. E. H. Love, *A Treatise on the Mathematical Theory of Elasticity*, 4th ed. (Dover, New York, 1927).
- [21] J. B. Keller, Surface tension force on a partly submerged body, *Phys. Fluids* **10**, 3009 (1998).
- [22] J. A. Nirody, J. Jinn, T. Libby, T. J. Lee, A. Jusufi, D. L. Hu, and R. J. Full, Geckos race across the water's surface using multiple mechanisms, *Curr. Biol.* **28**, 4046 (2018).